American Journal of Pathology, Vol. 167, No. 5, November 2005

Immunopathology and Infectious Diseases

Bacillus anthracis Edema Toxin Causes Extensive Tissue Lesions and Rapid Lethality in Mice

Aaron M. Firoved,* Georgina F. Miller,† Mahtab Moayeri,* Rahul Kakkar,‡ Yuequan Shen,§ Jason F. Wiggins,* Elizabeth M. McNally,‡ Wei-Jen Tang,§ and Stephen H. Leppla*

From the National Institute of Allergy and Infectious Diseases and the Division of Veterinary Resources,† Office of Research Services, National Institutes of Health, Bethesda, Maryland; and the Department of Medicine‡ and Ben May Institute for Cancer Research,§ The University of Chicago, Chicago, Illinois*

Bacillus anthracis **edema toxin (ET), an adenylyl cyclase, is an important virulence factor that contributes to anthrax disease. The role of ET in anthrax pathogenesis is, however, poorly understood. Previous studies using crude toxin preparations associated ET with subcutaneous edema, and ET-deficient strains of *B. anthracis* showed a reduction in virulence. We report the first comprehensive study of ET-induced pathology in an animal model. Highly purified ET caused death in BALB/cJ mice at lower doses and more rapidly than previously seen with the other major *B. anthracis* virulence factor, lethal toxin. Observations of gross pathology showed intestinal intralumenal fluid accumulation followed by focal hemorrhaging of the ileum and adrenal glands. Histopathological analyses of timed tissue harvests revealed lesions in several tissues including adrenal glands, lymphoid organs, bone, bone marrow, gastrointestinal mucosa, heart, and kidneys. Concomitant blood chemistry analyses supported the induction of tissue damage. Several cytokines increased after ET administration, including granulocyte colony-stimulating factor, eotaxin, keratinocyte-derived cytokine, MCP-1/JE, interleukin-6, interleukin-10, and interleukin-1β. Physiological measurements also revealed a concurrent hypotension and bradycardia. These studies detail the extensive pathological lesions caused by ET and suggest that it causes death due to multiorgan failure.** ***(Am J Pathol 2005, 167:1309–1320)***

The use of *Bacillus anthracis*, the causative agent of anthrax disease, as a bioweapon in October 2001 has led to a resurgence of scientific inquiry into mechanisms of anthrax pathogenesis. Greater knowledge of the physiological damage caused by the bacteria will aid in selection of appropriate interventions and supportive therapies. *B. anthracis* is a gram-positive, spore-forming rod able to resist harsh environmental conditions while retaining the ability to infect new hosts when inhaled, ingested, or exposed to breaks in the skin.[1] Inhalational anthrax patients often display fever, chills, nonproductive cough, and malaise.[2–6] Involvement of the gastrointestinal (GI) tract is indicated by nausea and vomiting. Although patients often present with normal heart rate and blood pressure, tachycardia and hypotension frequently develop as the disease progresses. Abnormal chest X-rays showing mediastinal widening and production of pleural effusions are a consistent and defining characteristic of inhalational anthrax.[2]

The bacterium relies on two major virulence factors, capsule and anthrax toxin, to evade the immune response and cause disease. Anthrax toxin is a tripartite toxin consisting of one receptor binding subunit, protective antigen (PA), and two catalytic subunits, lethal factor (LF) and edema factor (EF).[7–9] PA recognizes the cellular receptors capillary morphogenesis gene 2 (CMG2) and tumor endothelial marker 8 (TEM8) and is processed by the host protease furin. On formation of a heptamer, PA binds LF and/or EF. The complex is internalized via receptor-mediated endocytosis. Once the endosomal compartment acidifies, LF or EF is translocated to the cytosol. LF is a metalloprotease that cleaves members of the mitogen-activated protein kinase kinase (MAPKK) family leading to rapid cell lysis in murine macrophages from a limited number of inbred mouse strains.[10–12] EF is an adenylyl cyclase that converts ATP to cAMP, an impor-

Supported by the National Institutes of Health (to E.M.M., R.K., and GM53459, GM62548 and the Great Lakes Regional Center of Excellence pilot grants to W.J.T.), the American Heart Association (to E.M.M.), the Burroughs Wellcome Foundation (to E.M.M.), and the Intramural Research Program of the National Institute of Allergy and Infectious Diseases of the National Institutes of Health.

Accepted for publication July 18, 2005.

Address reprint requests to Stephen H. Leppla, Ph.D., Chief, Bacterial Toxins and Therapeutics Section, National Institute of Allergy and Infectious Diseases, National Institutes of Health, 30 Convent Dr., Building 30, Room 303, Bethesda, MD 20892-4349. E-mail: sleppla@niaid.nih.gov.

tant second messenger.[13] EF is at least 1000-fold more active than are host adenylyl cyclases in cAMP production.[14–16]

Many aspects of anthrax disease can be attributed to toxin function.[17,18] Lethal toxin (LT), composed of LF and PA, has been shown to induce vascular collapse and subsequent hypoxia-mediated toxicity in mice.[17] Hypoxia-mediated tissue necrosis in spleen, liver, and bone marrow is accompanied by pleural effusions, a hallmark of anthrax disease. However, LT toxicity does not account for other major pathophysiological lesions of anthrax disease such as renal dysfunction and hemorrhage of the GI tract, lymph nodes, or meninges.[4,19–22]

Pathological lesions resulting from ET-mediated toxicity have not been well studied. In cultured cell lines, ET has been shown to increase cAMP concentrations and induce Chinese hamster ovary cell rounding,[13] and to induce anti-inflammatory cytokines while suppressing lipopolysaccharide-mediated inflammatory cytokine release.[23,24] Mutant strains of *B. anthracis* lacking the gene for EF are attenuated in their virulence in a murine model when compared to a wild-type strain, albeit less so than a similar LF knockout.[25,26] Early studies of EF activity *in vivo* relied on toxin preparations from *B. anthracis* strains that not only produced EF but also LF, complicating interpretations of observed effects. Low concentrations of partially purified ET caused extensive edema in rabbits when injected subcutaneously. These ET preparations, however, caused less murine mortality when compared with a more crude preparation contaminated with LF.[27] More recent *in vivo* studies using purified ET have not been reported in any animal model. This deficiency primarily results from difficulty in obtaining the larger quantities of purified EF needed to perform detailed animal studies. Indeed, adenylyl cyclase toxins from other bacteria that share homology with ET, such as ExoY from *Pseudomonas aeruginosa*[28] or CyaA from *Bordetella pertussis*[29] have also been recalcitrant to large scale purification and have not been systematically studied in animal models.

Recently, the technical issues regarding EF purification have been resolved,[30] making possible a detailed study of ET effects *in vivo*. Surprisingly, we found that ET is highly lethal in a murine model at lower doses and more rapidly than has been shown previously for an equivalent dose of LT.[17,31] Further, ET induced many lesions that occur in anthrax disease. These lesions are distinct from those induced by LT intoxication, including lymph node and focal GI tract hemorrhaging.[22,32] Histopathological analyses revealed diverse tissue damage to several organs including the adrenal gland, which could in turn explain some of the effects seen in other tissues. We present here the first report of histopathological and physiological effects of ET in mice.

Materials and Methods

Toxin

PA was purified from *B. anthracis* culture supernatants[33] and N-terminal His-tagged EF proteins were purified from *Escherichia coli* as previously described.[30] EF-K346R, a mutant form of EF with 10,000-fold less catalytic activity, was made by introducing the indicated amino acid substitution to the EF expression plasmid using the QuickChange site-directed mutagenesis kit from Stratagene (La Jolla, CA). Assays with the Limulus Amebocyte Lysate 120 test kit (Cambrex, East Rutherford, NJ) showed the EF preparations contained ≤10 pg of lipopolysaccharide/μg of EF produced. All toxin preparations were diluted in filter-sterilized 1× phosphate-buffered saline (PBS), frozen, and thawed only once before use. Doses of toxin refer to the amount of the EF component with PA added at the same amount (ie, 100 μg of ET is 100 μg of EF plus 100 μg of PA).

Animals

Female 10- to 12-week-old BALB/cJ mice (The Jackson Laboratory, Bar Harbor, ME) were injected intravenously (100 μl) or intraperitoneally (500 μl) with sterile 1× PBS, EF, or ET. All protocols were approved by the National Institute of Allergy and Infectious Diseases Animal Care and Use Committee.

Survival Curves

Groups of three to five animals received intravenous injections of various doses of ET or EF. Animals were assessed for viability every 4 hours after injection. Duplicate experiments were combined, and survival curves were compared by the log-rank test.

Histopathology and Serum Chemistry

Groups of mice were intravenously injected with 37.5 μg of ET ($n = 28$) and, as controls, either EF alone ($n = 4$) or PBS ($n = 5$). Three ET-injected mice that best represented the observable physiological status of the group as a whole and one control animal that received either ET or PBS, for a combined total of six control animals, were chosen at 2.5, 12, 24, 36, and 48 hours. Animals were first bled by cardiac puncture while anesthetized with isoflurane, USP (Forane; Baxter Health Care Corp., Deerfield, IL), using an EZ-1000 fixed small animal anesthesia system (Euthanex Corp/, Palmer, PA). Mice were then immediately euthanized by carbon dioxide inhalation and necropsied. The following tissues were harvested and fixed in 10% buffered formalin phosphate (Fisher Scientific, Inc., Fairlawn, NJ): skin, salivary glands (submandibular, sublingual, parotid), tongue, pancreas, lymph nodes (cervical, inguinal, auxiliary, mesenteric), thymus, adrenal glands, thyroid glands, pituitary gland, sciatic nerve, brachial plexus, skeletal muscle, eyes, Harderian glands, GI tract, liver, spleen, lungs, trachea, esophagus, heart, kidneys, uterus, ovaries, urinary bladder, brain, stifle joint with attached distal femur and proximal tibia, nares, skull, teeth, inner and middle ears, spinal cord, vertebrae, and dorsal root ganglia. After fixation, tissues were processed for routine paraffin embedding, sectioned, and stained with hematoxylin and eosin or Alcian Blue (pH 2.5) (His-

toserv, Inc., Germantown, MD).[34] Serum analyses were performed within 2 hours of blood collection using the VetACE clinical chemistry system (Alfa Wassermann, Inc., West Caldwell, NJ) for albumin, amylase, blood urea nitrogen, calcium, glucose, inorganic phosphorus, total protein, alkaline phosphatase, γ-glutamyl transferase, lactate dehydrogenase, alanine aminotransferase, aspartate aminotransferase, and total bilirubin. Hematological analyses were performed using a Hemavet 1500FS blood analyzer (CDC Technologies, Oxford, CT). Normal ranges for serum chemistries and hematological analyses were established previously on the analyzer using >50 mice. Blood smears were also prepared from ethylenediamine tetraacetic acid-treated blood using a Diffspin DS02 (Statspin, Inc., Norwood, MA) and stained with Three Step stain (Richard-Allan Scientific, Kalamazoo, MI). A veterinary pathologist certified by the American College of Veterinary Pathologists (G.F.M.) evaluated the slides using an Olympus BX41 compound binocular microscope (Olympus America Inc., Melville, NY). Lesions were graded as minimal, mild, moderate, or severe.

Cytokine Analysis

Serum cytokine levels were assayed by Bio-Plex Mouse Cytokine 18-Plex Panel assay (Bio-Rad Laboratories, Inc., Hercules, CA) or enzyme-linked immunosorbent assay (ELISA) (Quantikine; R&D Systems Inc., Minneapolis, MN). For Bio-Plex assays, three mice at each time point were injected intravenously with ET (37.5 μg). Control animals at each time point consisted of three animals injected with either EF (37.5 μg) or PBS. Mice were anesthetized with isoflurane and bled by cardiac puncture at 1, 4, 6, 12, 18, 24, 36, and 48 hours after injection. Collected blood was allowed to clot for 1 to 2 hours and centrifuged in serum separator tubes (Sarstedt Inc., Newton, NC). Sera were frozen, stored at −80°C, and thawed once to assay according to the manufacturer's instructions. Samples from two independent time course experiments were run in duplicate on the Luminex 100 IS system (Luminex Corp., Austin, TX) by the National Institute of Allergy and Infectious Diseases Research and Technology Branch core facility (National Institutes of Health, Bethesda, MD). For ELISA analyses, six to nine ET-treated or control animals were bled 1, 6, 12, 18, 24, 30, and 48 hours after intravenous injection and processed as previously described. Pools of serum from two animals were assayed in duplicate for levels of interleukin (IL)-1α, IL-1β, IL-6, IL-10, MCP-1/JE, eotaxin, keratinocyte-derived cytokine (KC), tumor necrosis factor (TNF)-α, MIP-1α, and granulocyte colony-stimulating factor (G-CSF) by ELISA using the manufacturer's protocols with modification in serum dilutions to ensure measurements were made in the range of the standards.

Telemetry Measurements

Radio frequency devices were implanted for independent monitoring of blood pressure or heart rate using devices from Data Sciences Int. (St. Paul, MN) as described.[35] Briefly, mice were anesthetized with isoflurane and either a blood pressure or a heart rate monitor was implanted. Blood pressure recording devices were implanted via a carotid approach into the aorta. Heart rate monitoring devices were implanted subcutaneously on the dorsum with the leads in an electrocardiogram lead II position. Mice were allowed to recover from surgery for 24 hours before exposure to ET. ET (100 μg) was intraperitoneally injected and recordings were made. Blood pressure and heart rate recordings were compared before and after exposure to ET.

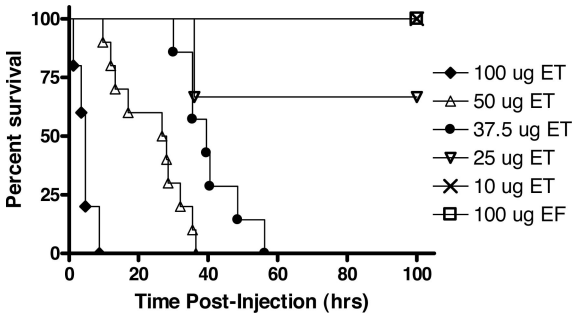

Figure 1. ET lethality in BALB/cJ mice. ET-treated female BALB/cJ mice at doses of 100 μg ($n = 5$), 50 μg ($n = 10$), 37.5 μg ($n = 7$), 25 μg ($n = 6$), and 10 μg ($n = 6$), were compared to animals treated with 100 μg of EF alone (control). All injections were intravenous in 100-μl volume. All differences in survival curves when compared against each other were statistically significant ($P < 0.05$) by the log-rank test except for the comparison between the 25 μg of ET dose and 100 μg of EF dose ($P = 0.1573$).

Statistics

Graphs and statistics were generated with GraphPad PRISM 4.0 software (GraphPad Software, Inc., San Diego, CA).

Results

Effects of ET Dosage on Murine Mortality

An initial examination of ET toxicity in female BALB/cJ mice was performed with an intravenous injection of 100 μg of ET (100 μg of EF + 100 μg of PA), analogous to a dose used previously for LT studies (100 μg of LF + 100 μg of PA).[17] Within 5 minutes, mice exhibited a languid behavior with little ambulatory movement and generally assumed a sprawled prone position. Animals recovered slightly but remained hunched and became increasingly lethargic with time. Mortality in all animals occurred within 9 hours (Figure 1 and data not shown). In experiments using 100 μg of ET to compare routes of inoculation, the median survival time after intravenous injection (6 hours) was approximately one third of that after intraperitoneal injection (21 hours) (Supplemental Figure 1, see *http://ajp.amjpathol.org*). Decreasing the ET dose to 50 μg yielded a longer median survival time for the intravenous route and complete survival for those inoculated by the intraperitoneal route.

More extensive dose curves were obtained for BALB/cJ mice given toxin by the intravenous route (Fig-

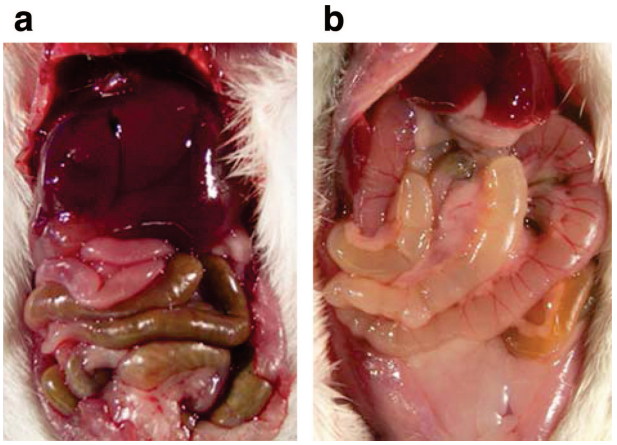

Figure 2. ET induces marked intestinal dilatation. Mice were injected intravenously with 37.5 μg of EF alone (control) (**a**) or ET (**b**) and euthanized 12 hours later by CO_2 inhalation and immediately necropsied.

ure 1). A dose-dependent response was observed. At 50 and 37.5 μg of toxin, median survival times were 27 and 40 hours, respectively, with mortality occurring in all animals. Only two of six animals receiving 25 μg of ET died, although all animals exhibited signs of illness. A dose of 10 μg of ET resulted in minimal morbidity and no mortality. Injection of EF in the absence of PA at doses up to 100 μg did not result in any symptoms, similar to controls receiving a PBS injection. Previous studies have shown PA alone to be nontoxic.[17]

Gross Pathology of ET-Treated Mice

To allow for the development of significant pathological changes, an intermediate intravenous dose of 37.5 μg of ET was chosen. Female BALB/cJ mice received ET, PBS, or EF alone. Animals that received EF were indistinguishable from PBS-treated mice and exhibited no gross lesions at any time point, indicating that the EF preparation itself did not cause any abnormal pathologies. The first gross pathology observed in ET-treated animals was copious fluid accumulation in the lumen of the intestines (Figure 2). Fluid in the intestinal lumen was present from the earliest time point of 2.5 hours and was observed as early as 1 hour in other studies (data not shown). Focal hemorrhaging into the lumen of the cecum was seen beginning at 24 hours with hemorrhagic content observed in the intestine and stomach. Hemorrhaging was also observed by 12 hours in the adrenal glands, often restricted to the right adrenal gland but occasionally involving the left adrenal at later time points. This unilateral lesion is similar to posttraumatic adrenal hemorrhage in which pressure fluctuations due to outflow obstruction of the draining inferior vena cava by direct compression or thrombosis more often affects the right adrenal.[36] The marked intestinal dilatation induced by ET may provide the necessary obstruction of the inferior vena cava leading to hemorrhage of the right adrenal. Hemorrhaging into the mesenteric lymph nodes and ovaries was occasionally noted. Pleural effusions associated with anthrax disease and seen in LT-treated animals were absent.[17,21]

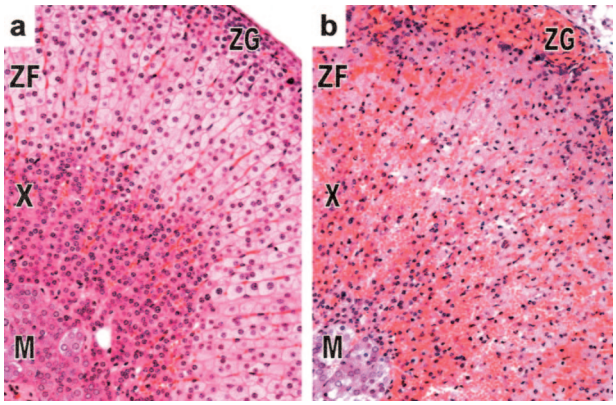

Figure 3. ET causes adrenal gland lesions. Histopathological evaluation of adrenal glands at 12 hours in EF-treated (control) (**a**) and ET-treated (**b**) animals revealed necrosis and hemorrhage of the zona fasciculata (ZF) of the adrenal cortex induced by ET. The X-Zone (X) and zona glomerosa (ZG) were moderately necrotic whereas the medulla (M) was minimally affected by ET. Original magnifications, ×20.

Histopathology Findings

Widespread histopathological lesions were observed in disparate organs including the adrenal glands, lymphoid organs, bone, bone marrow, GI mucosa, heart, kidneys, reproductive tract mucosa and follicular cells, and submandibular glands. Unlike *B. anthracis* infections in humans or primates,[21,22] we observed no lesions of the liver or brain meninges. No lesions were observed in mice treated with PBS or EF.

Adrenal Gland

Significant histopathological lesions in the adrenal gland were first observed at 12 hours after toxin injection. A diffuse coagulative moderate to severe necrosis of the corticosteroid-producing zona fasciculata in the adrenal cortex accompanied by granulocytic infiltrates was observed by 12 hours and became severe by 24 hours (Figure 3b). The zona glomerulosa and X-zone, a region unique to mice, were moderately necrotic. The medulla was minimally affected, if at all. Lesions remained consistent throughout all subsequent time points with no evidence of regeneration.

Lymphoid Organs

Mild lymphocytolysis, characterized by the presence of karyorrhetic debris, was present by 12 hours in all examined lymphoid tissue, including lymph nodes, thymus, spleen, and gut-associated lymphoid tissue (Figure 4). Lymphocytolysis increased by 36 hours to a moderate to severe level of lymphoid depletion. While lymphocytes of the thymus underwent lysis (Figure 4b), the underlying reticular epithelial cells and medulla were unaffected. The periarteriolar lymphoid sheaths forming the splenic white pulp (Figure 4d) showed necrotic lesions similar to those observed in the thymus with more mild effects occurring in the red pulp. In addition to depletion of more matured lymphoid cells, progenitor cells of the femoral

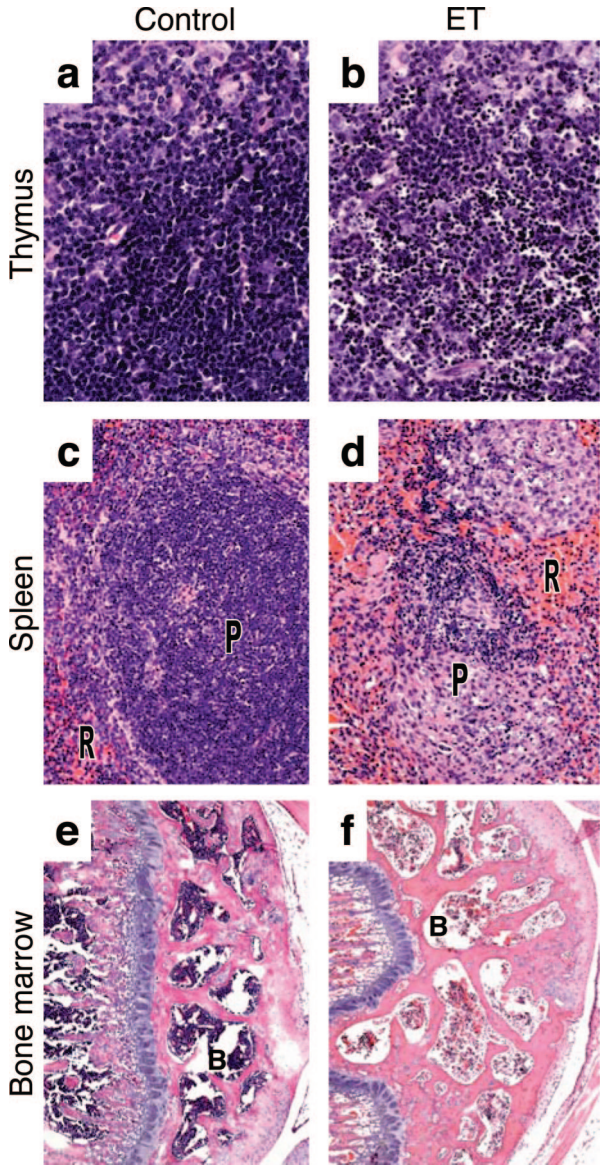

Figure 4. Histopathological analysis of lymphoid tissues. Mice were injected intravenously with 37.5 μg of EF alone (control), PBS, or 37.5 μg of ET before histopathological analysis of lymphoid tissues. **a:** Thymus from EF-treated (36 hours) control. **b:** Nuclear fragmentation of lymphocytes in the thymus of ET-treated animals (36 hours). **c:** Red pulp (R) and periarteriolar lymphoid sheath (P) of spleen of PBS-treated (48 hours) control. **d:** Necrotic splenic periarterial lymphoid sheath in ET-treated (48 hours) animals. **e:** Bone marrow (B) in PBS-treated (48 hours) control. **f:** Depletion of hematopoietic cells of the bone marrow in ET-treated mice (48 hours). Original magnifications: ×40 (**a**, **b**); ×20 (**c**, **d**); ×5 (**e**, **f**).

bone marrow were mildly depleted (Figure 4f) at 24 hours and moderately depleted at 36 and 48 hours although few necrotic cells were noted.

Bone

Moderate condensation and fragmentation of nuclei with accompanying cell loss occurred at 24 hours in osteoblasts and osteocytes of the metaphyseal trabeculae of the femur and tibia (Figure 5b). Occasional osteoblasts in the epiphysis and diaphysis were necrotic, but the osteocytes in these locations appeared unaffected.

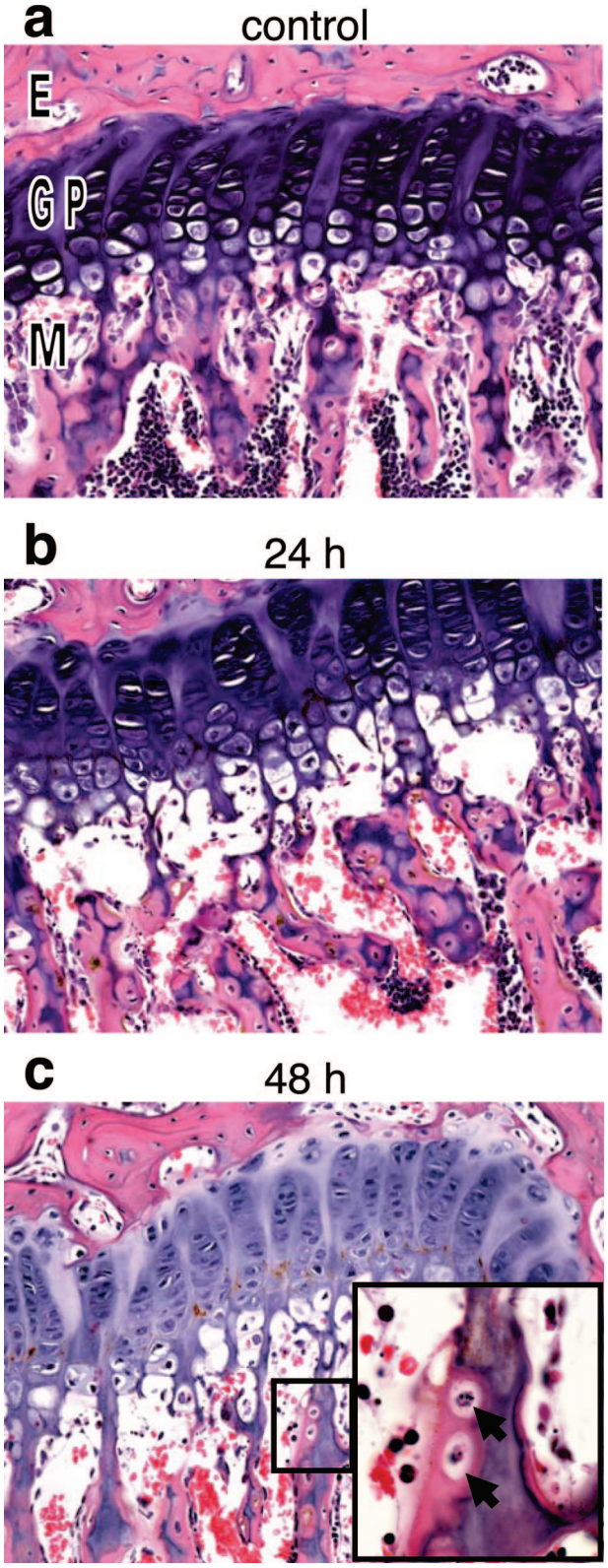

Figure 5. Bone degeneration after ET administration. Histopathological analysis of femur after intravenous injection with 37.5 μg of EF (control), PBS, or 37.5 μg of ET. **a:** Growth plate from femur of PBS control (24 hours). **b** and **c:** Loss of osteoblasts and osteocytes of the metaphyseal bone marrow at 24 (**b**) and 48 (**c**) hours after ET treatment. **Inset**: Lacunae containing necrotic osteocytes (**solid arrows**). E, epiphysis; GP, growth plate; M, metaphysis. Original magnifications: ×20; ×100 (**inset**).

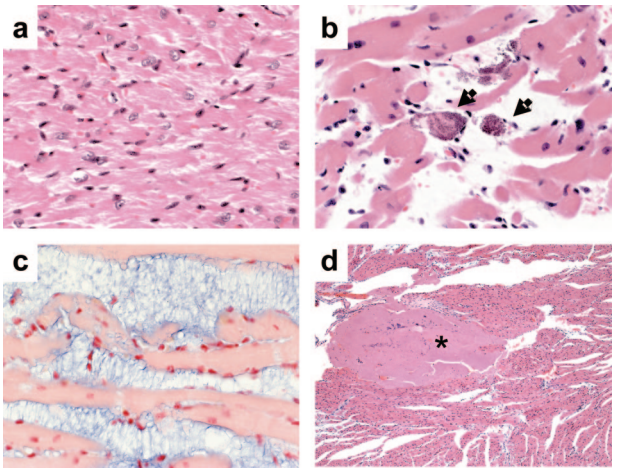

Figure 6. ET-induced cardiac damage. Histopathological analysis of cardiac tissues after intravenous injection with 37.5 μg of EF, PBS, or 37.5 μg of ET. **a:** Cardiomyocytes from PBS-treated (48 hours) control. **b:** Cardiomyocyte degeneration in ET-treated mice (**arrows**, 48 hours). **c:** Interstitial myxoid deposits in heart tissue stained with Alcian blue (48 hours). **d:** Thrombus formation at 12 hours after ET-treatment (**asterisk**). Original magnifications: ×40 (**a–c**); ×5 (**d**).

By 48 hours, there was loss of metaphyseal bone, with partial discontinuity between the osseous trabeculae and the differentiating epiphyseal chondrocytes. There was no evidence of osteoblast regeneration and no increased osteoclastic activity through 48 hours.

Heart

Mild cardiac lesions were evident at 12 hours in a multivessel distribution with coronary cardiomyocytes multifocally separated. At 24 hours, the heart was moderately affected with rare cardiomyocyte degeneration (Figure 6b) and increased separation of myofibers. The cardiomyocyte interstitial space was filled with a myxoid ground substance deposit that stained blue with the proteoglycan Alcian blue stain (Figure 6c). Multifocally extensive areas of cardiomyocyte necrosis were observed and interfiber myxoid accumulation increased at 36 and 48 hours. Additionally, by 12 hours platelet/fibrin thrombi were found within coronary vessels, the ventricular lumen, and attached to the endothelium (Figure 6d).

Gastrointestinal Tract

Mild intralumenal hemorrhage of the GI tract and multifocal necrosis of the stomach (Figure 7a), intestine (Figure 7b), and cecum mucosa was observed at 12 hours. Patchy mucosal necrosis of these organs was found in the mucosal layer and may be due to underlying thrombi without affecting adjacent crypt cells. Lesions became severe at 24 hours but returned to a mild to moderate level at 36 and 48 hours. Deposition of fibrin or platelets was observed at 12 hours within villar tips of the small intestine (Figure 7c), presumably within the capillary, peaking in severity at 36 hours. Surprisingly, the intestinal wall did not appear edematous despite the marked fluid accumulation within the lumen of the intestine.

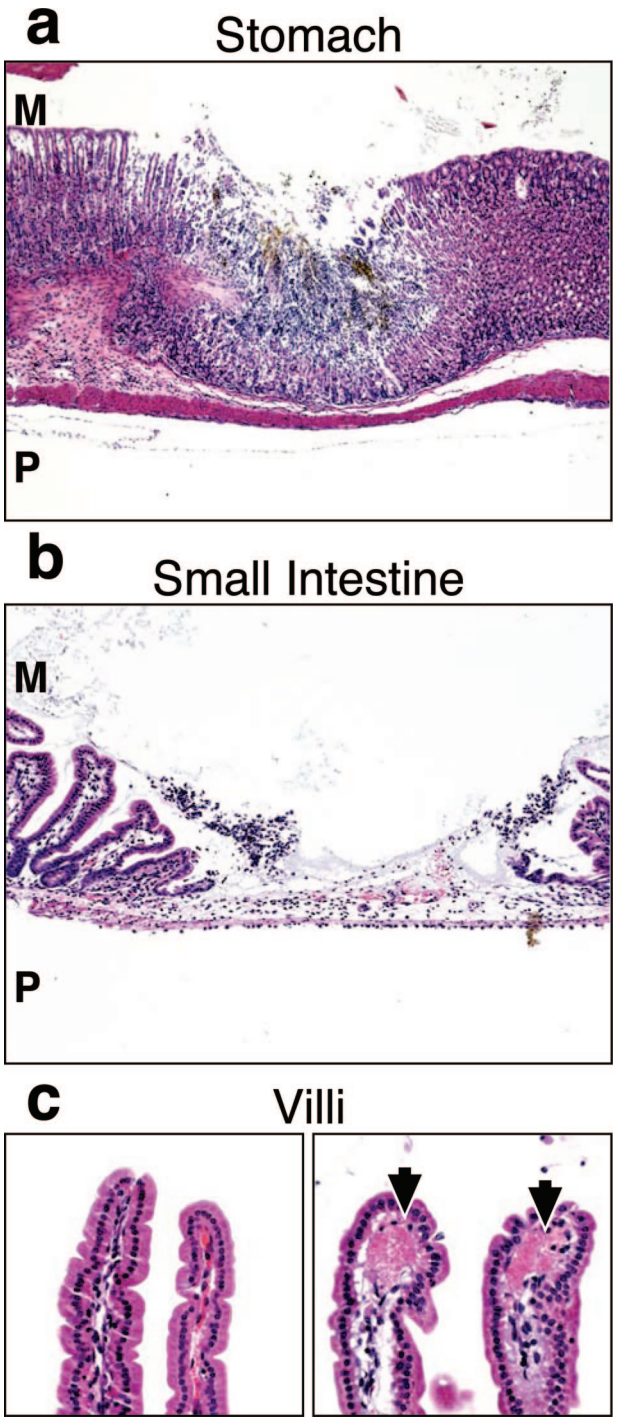

Figure 7. Fibrin deposition and mucosal degeneration of GI tract caused by ET. Histopathology of GI tract mucosa after intravenous injection with 37.5 μg of EF, PBS, or 37.5 μg of ET. **a:** Areas of focal necrosis surrounded by normal tissue in the stomach mucosa of ET-treated mice (36 hours). **b:** Focal necrosis of the intestine 24 hours after ET treatment. **c:** Fibrin deposition in the villus tips in ET-treated animals (24 hours; **right**, **arrows**) as compared to normal villi from control animals (24 hours, **left**). M, mucosal surface; P, peritoneal cavity. Original magnifications: ×5 (**a**); ×10 (**b**); ×20 (**c**).

Other Microscopic Observations

Additional organs displayed histopathological lesions after ET administration (Supplemental Figures 2 to 5, see *http://ajp.amjpathol.org*). The kidney was mildly affected

Table 1. Serum Chemistry

	Normal range	Controls*	ET treated†				
			2.5 hours	12 hours	24 hours	36 hours	48 hours
ALT (U/L)	13 to 109	50 ± 19	205 ± 57‡	213 ± 54‡	144 ± 32‡	229 ± 73‡	98 ± 29‡
AST (U/L)	31 to 224	114 ± 57	453 ± 137‡	549 ± 17‡	378 ± 47‡	531 ± 154‡	409 ± 141‡
LDH (U/L)	54 to 658	295 ± 100	1284 ± 461‡	2176 ± 263‡	2057 ± 321‡	>3200§	>3200§
BUN (mg/dl)	13 to 37	18 ± 1	35 ± 3‡	91 ± 2‡	146 ± 55‡	149 ± 56‡	>200§
Bilirubin (mg/dl)	0 to 0.8	0.32 ± 0.08	0.43 ± 0.06	0.37 ± 0.06	0.70 ± 0.20‡	0.83 ± 0.21‡	0.70 ± 0.28‡
GGT (U/L)	0 to 37	0	1.0 ± 1.0	1.33 ± 0.6‡	19.0 ± 5.2‡	14.0 ± 5.6‡	3.5 ± 5.0
Protein, total (g/dl)	4.2 to 5.8	4.5 ± 0.2	4.3 ± 0.5	3.7 ± 0.5‡	3.6 ± 0.3‡	3.7 ± 0.6‡	3.25 ± 0.1‡
ALP (U/L)	6 to 251	213 ± 25	190 ± 13	192 ± 50	270 ± 32‡	307 ± 67‡	317 ± 25‡
Phosphorus (mg/dl)	4 to 11	9 ± 1	7 ± 1	15 ± 2‡	31 ± 7‡	23 ± 7‡	21 ± 1‡
Calcium (mg/dl)	7.6 to 9.7	9.1 ± 0.2	6.3 ± 0.5‡	8.0 ± 0.7‡	5.7 ± 0.9‡	5.3 ± 0.4‡	4.8 ± 0.2‡
Glucose (mg/dl)	115 to 323	229 ± 37	348 ± 66‡	135 ± 24‡	64 ± 8‡	75 ± 32‡	112 ± 28‡
Amylase (U/L)	509 to 1272	488 ± 51	413 ± 72	1062 ± 391‡	1943 ± 430‡	2785 ± 498‡	1311 ± 425‡

*Average and standard deviation of six animals.
†Average and standard deviation of three animals per time point except at 48 hours ($n = 2$).
‡Mean significantly different ($P < 0.05$) by unpaired *t*-test from control group in this experiment and may fall within the normal range.
§Value was above maximal assay dilution.

at 12 hours, displaying cytoplasmic vacuolation in scattered cortical tubular epithelial cells with occasional necrotic cells (Supplemental Figure 2, see *http://ajp.amjpathol.org*). Renal lesions became moderate from 24 to 48 hours. Submandibular salivary gland acinar cells were mildly swollen, with microvesicular vacuolation of the cytoplasm by 24 hours (Supplemental Figure 3, see *http://ajp.amjpathol.org*). The ovaries displayed increased numbers of atretic follicles at 24 hours, and the ovum within most tertiary follicles appeared mildly to moderately degenerate from 12 hours onward. Thecal cells within affected tertiary follicles were generally hyperchromatic and lacked normal cohesiveness (Supplemental Figure 4, see *http://ajp.amjpathol.org*). By 12 hours, several of the treated mice and none of the control mice had minimal to moderate uterine epithelial degeneration not expected at their stage of estrus (Supplemental Figure 5, see *http://ajp.amjpathol.org*).

Serum Chemistries in ET-Treated Mice

Analysis of markers for cellular leakage in serum of ET-inoculated animals indicated widespread tissue damage (Table 1).[37] The cytosolic enzymes alanine aminotransferase, aspartate aminotransferase, and lactate dehydrogenase increased by 2.5 hours and remained elevated above those for control animals through 48 hours, indicative of damage to cell membranes in multiple organs, including intestine, kidney, and heart.

Several additional markers with aberrant serum levels provide an initial survey of organ systems that potentially respond to ET administration. Blood urea nitrogen concentration was elevated by 2.5 hours and continued to increase through 48 hours. Although this may be a result of renal insufficiency, it could also be due to dehydration, hemorrhaging, or simply reflective of the increased protein load due to intestinal dysfunction. Definitive determination of kidney dysfunction will require testing for other markers. Inorganic phosphorus was elevated in all mice from 2.5 hours onward and may be due to release of intracellular phosphate by cell lysis or renal failure. The low calcium levels may be in response to the observed hyperphosphatemia. Total protein serum levels were below reference range from 12 hours onward and could be the result of congestive heart failure, liver disorders, or hemorrhaging. An increase in alkaline phosphatase peaking at 36 hours was potentially indicative of hepatic biliary obstruction or bone damage. Bilirubin and γ-glutamyl transferase levels increased greater than controls although they remained within normal ranges. Serum glucose levels, which can be influenced by stress, starvation, or glucocorticoid function, were elevated at 2.5 hours but were low at 24 and 36 hours. Serum amylase, which in the mouse is primarily of salivary gland origin, was elevated by 12 hours and is likely the result of the observed perturbation of the acinar cells of the submandibular gland. Significant changes were not seen in albumin, triglycerides, or uric acid levels (data not shown).

Hematology

Hematology analyses (Table 2) revealed a sustained increase of monocytes and neutrophils beginning by 2.5 hours in ET-treated animals that remained elevated through 48 hours. These results may reflect mobilization of these cell types from bone marrow or lymphoid organs, as supported by the observed depletion of pluripotent stem cells from the bone marrow (Figure 4f). Additionally, examination of blood smear preparations revealed that the circulating monocytes were often hypervacuolated (Supplemental Figure 6, see *http://ajp.amjpathol.org*). No other hematological parameters examined exhibited significant changes outside of normal ranges.

Serum Cytokine Response in ET-Treated Mice

Edema toxin has been shown to modulate cytokine expression by inducing IL-6 but not TNF-α in the RAW264.7 macrophage cell line and is able to inhibit lipopolysaccharide-stimulated TNF-α production.[23,24] To determine whether ET affects the cytokine profile *in vivo*, female

Table 2. Hematology

	Normal range	Controls*	ET Treated†				
			2.5 hours	12 hours	24 hours	36 hours	48 hours
Monocytes (K/μL)	0.01 to 0.52	0.09 ± 0.12	0.24 ± 0.09	0.58 ± 0.49	0.71 ± 0.55‡	0.81 ± 0.57‡	1.58 ± 1.02‡
Neutrophils (K/μL)	0.001 to 2.52	0.57 ± 0.72	1.75 ± 0.75	3.44 ± 0.73‡	2.55 ± 1.31‡	3.13 ± 0.56‡	3.51 ± 2.65‡
Lymphocyte (K/μL)	0.36 to 4.46	1.53 ± 1.02	0.78 ± 0.28	1.33 ± 0.43	3.09 ± 2.67	1.30 ± 1.02	1.64 ± 1.10
WBC (K/μL)	0.6 to 6.38	2.2 ± 1.0	2.8 ± 0.9	4.8 ± 1.0‡	6.4 ± 1.2‡	5.3 ± 2.1‡	6.7 ± 3.1‡
Platelets (K/μL)	532 to 1300	557 ± 261	651 ± 102	421 ± 10.4	492 ± 244	153 ± 32‡	246 ± 158
RBC, total (M/μL)	7.7 to 10.1	7.8 ± 0.3	8.9 ± 0.3‡	9.0 ± 0.8‡	9.0 ± 0.6‡	8.3 ± 0.9	8.7 ± 0.4‡
Hematocrit (%)	36.8 to 49.1	40.0 ± 2.3	44.2 ± 1.8‡	46.3 ± 5.3‡	45.6 ± 3.9‡	44.0 ± 6.2	44.3 ± 3.0‡
Hemoglobin (g/dl)	12.3 to 15.6	12.3 ± 0.3	14.2 ± 0.3‡	14.5 ± 1.3‡	14.0 ± 1.1‡	12.9 ± 1.7	13.3 ± 0.5‡
MCV (fl)	43.6 to 53.27	51.0 ± 1.1	49.7 ± 0.5	51.7 ± 3.4	50.8 ± 1.3	52.7 ± 2.3	50.9 ± 1.8

Units: K, thousand cells; M, million cells.
*Average and standard deviation of six animals.
†Average and standard deviation of three animals per time point.
‡Mean significantly different ($P < 0.05$) by unpaired t-test from control group in this experiment and may fall within the normal range.

BALB/cJ mice were injected with 37.5 μg of ET, EF, or PBS and serum was collected at multiple time points. Initially, sera were analyzed for 18 cytokines using a multiplex assay, and no appreciable induction of IL-2, IL-3, IL-4, IL-17, TNF-α, or interferon-γ was seen in repeated experiments. The remaining cytokines showed some induction but often to variable levels (data not shown). Selected cytokines were then assayed by ELISA. Pooled sera from two to three animals at each time point were assayed in duplicate for IL-1α, IL-1β, IL-6, IL-10, eotaxin, G-CSF, MCP-1/JE, KC, MIP-1α, and TNF-α (Figure 8). Early induction followed by a decline with time in serum levels was observed for G-CSF, eotaxin, and KC. The highest ET-induced cytokine, G-CSF, was present in sera (up to 200 ng/ml) at 4000-fold background (PBS- or EF-treated) levels. A bimodal response with an initial spike in cytokine expression followed by a decline before a second increase in terminally ill animals was observed in IL-6, MCP-1/JE, and IL-1α. IL-10 showed a modest increase that stayed elevated throughout all time points.

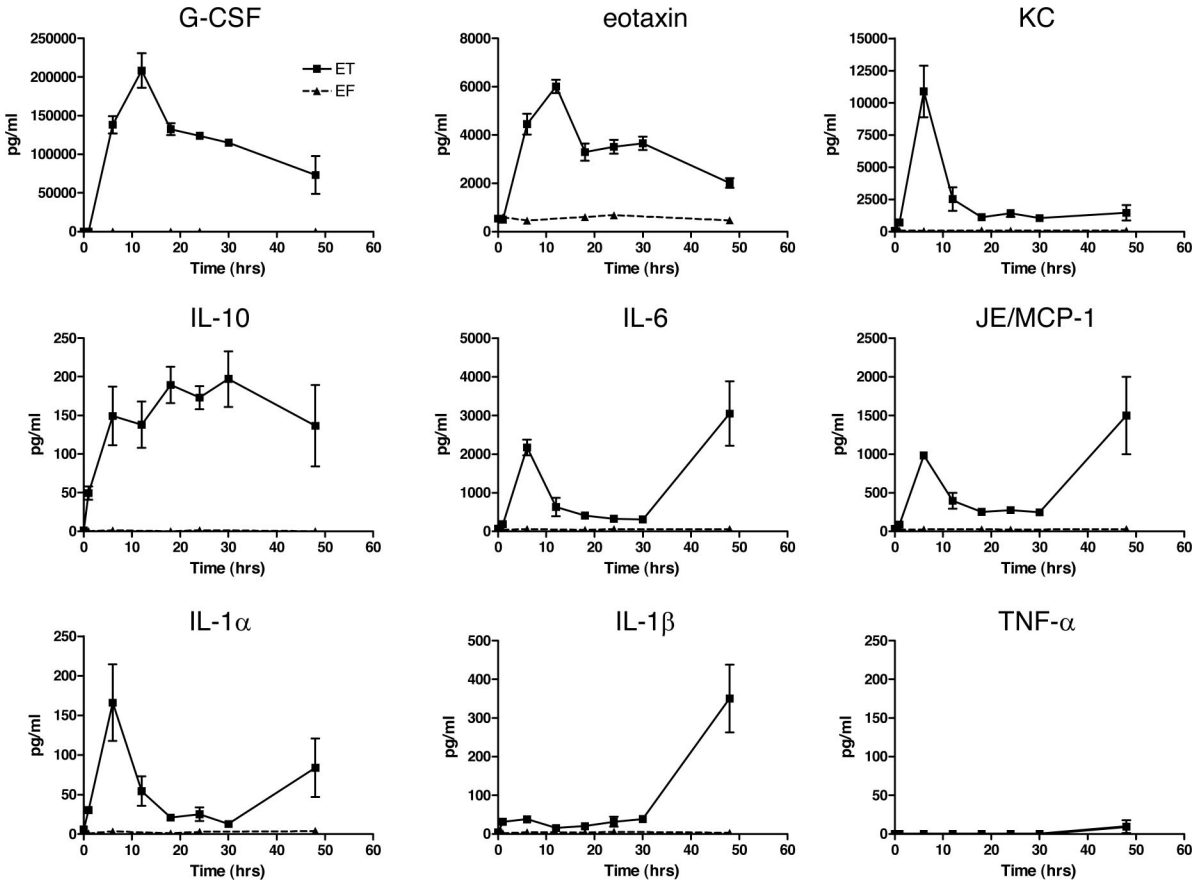

Figure 8. ET-induced cytokine response. Measurements of serum cytokine levels after intravenous injection of 37.5 μg of ET or EF (control). Results represent averages from duplicate measurements done on three pools of sera, each deriving from two mice except for the 48-hour ET-treated animals in which duplicate measurements were done on sera drawn from three individual animals.

No appreciable induction was shown for TNF-α (Figure 8) or MIP-1α (data not shown). The absence of a cytokine response to injections of EF alone also demonstrated the negligible contribution any residual lipopolysaccharide contamination makes in our system.

Blood Pressure/Rate/Electrocardiogram Telemetry Measurements

Radiofrequency recordings of blood pressure and heart rate were made after intraperitoneal injection of 100 μg of ET, a dose expected to produce 50% mortality at 18 hours (Supplemental Figure 1, see *http://ajp.amjpathol.org*). Both hypotension and bradycardia developed in mice within 1 hour after exposure to ET (Figure 9A). The rapid onset of bradycardia and the absence of tachycardia are consistent with a primary effect of ET on the heart. The dominant underlying heart rhythm associated with ET-induced hypotension and bradycardia remained sinus rhythm with mild widening of the QRS complex. Four hours after ET exposure, atrioventricular heart block could be seen (Figure 9B). Control animals that received mutated ET (PA + EF K346R) that has greater than 1000-fold reduced adenylyl cyclase activity exhibited no drop in arterial blood pressure (Figure 9C).

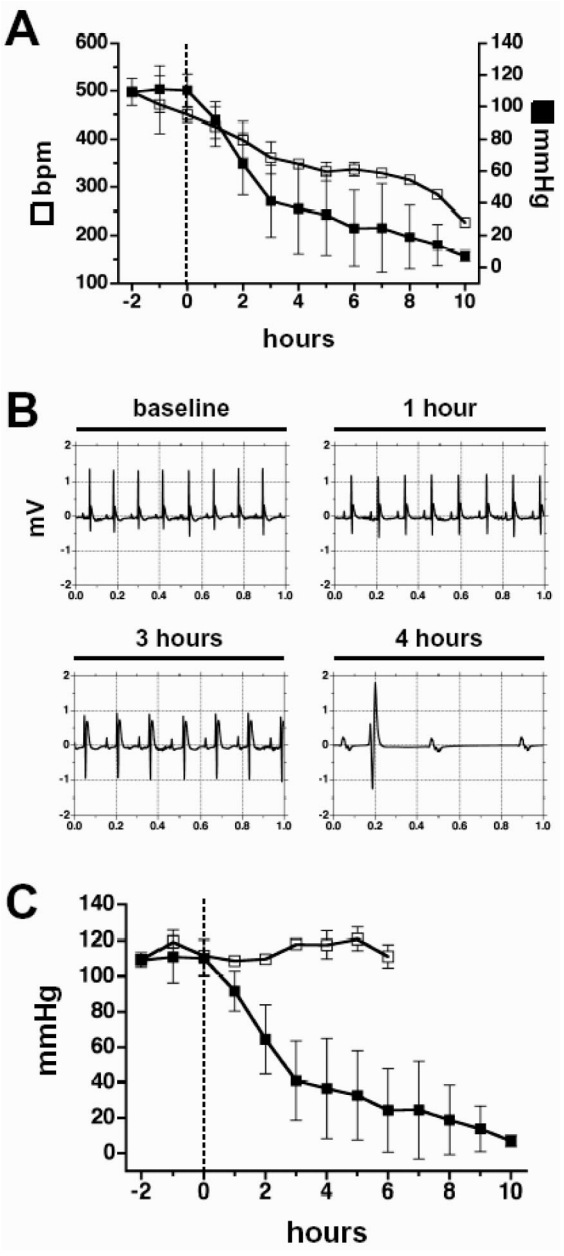

Figure 9. Cardiovascular response to ET exposure. **A:** Mean heart rate (bpm, **open boxes**) and arterial blood pressure response (mmHg, **filled boxes**) after intraperitoneal ET (100 μg) injection (n = 4). The **dashed line** represents the time of injection. Both heart and blood pressure declined simultaneously. **B:** Representative electrocardiogram tracings at baseline and timed intervals after exposure to ET. QRS widening and heart block can be seen at 4 hours after ET exposure. **C:** Constant mean arterial blood pressure after intraperitoneal injection of 100 μg of mutant E346R ET (n = 2, **open boxes**) as compared to native ET (n = 4, **filled boxes**) plotted in **A**.

Discussion

The studies presented here provide the first detailed analyses of toxicity induced by purified ET in an animal model. ET rapidly causes death in BALB/cJ mice. Toxin-treated animals displayed copious intestinal intralumenal fluid accumulation accompanied by hemorrhage into the lumen of the GI tract. Histopathological and blood chemistry analyses revealed extensive organ damage. Bradycardia and vascular collapse, accompanied by necrotic lesions and thrombi formation in the heart, resulting in cardiac failure, may represent the final events comprising ET-mediated death.

A striking observation in these studies was the rapidity with which ET incapacitates and leads to death of challenged mice. Within 5 to 20 minutes, depending on the administered dose, animals exhibited decreased mobility and increased difficulty in breathing. Mortality resulted as rapidly as 4 to 5 hours at the highest dose examined. A comparable molar dose of LT has a median survival time of 48 to 60 hours with no significant signs of illness occurring until 12 hours before death.[17,31] Thus, the application of the descriptive terms "lethal" and "edema" may understate the full consequences of these toxins *in vivo*. The combination of EF and PA may be better described in the future as "adenylyl cyclase toxin" to bring the terminology more in line with its counterparts in other bacterial species.

The administration of ET to mice resulted in a wide range of lesions striking disparate organs as might be expected for a toxin for which its receptors show a wide tissue distribution and that results in the excessive production of the critical second messenger cAMP. General tissue damage was corroborated by leakage of several cytosolic enzymes. A study examining clinical features of human inhalational anthrax[3] was remarkably consistent with serum chemistry trends observed for ET-treated mice. Most of the inhalational anthrax patients examined presented with high aspartate aminotransferase, alanine aminotransferase, and blood urea nitrogen levels, as well as low albumin and calcium levels. A smaller percentage

of patients exhibited high hematocrit or hemoglobin levels and elevated bilirubin levels.

After ET administration, extensive intestinal fluid accumulation was observed in the lumen of the GI tract, reminiscent of the large volumes of watery secretions during cholera infection resulting from the activation of host adenylyl cyclase activity by cholera toxin.[38] Additionally, necrotic lesions were observed in the GI mucosa, heart, adrenal glands, bone, kidney, and reproductive organs. Vacuolization was also a common observation, occurring in acinar cells of the submandibular gland, renal tubular epithelial cells, and circulatory monocytes. Notably, overt hepatic lesions were absent in ET-treated animals, suggesting that low serum protein levels, elevated alkaline phosphatase, and slight increases in bilirubin and γ-glutamyl transferase might result from other causes, possibly hemorrhage or bone necrosis. Other lesions observed during inhalational anthrax disease, such as pulmonary epithelial cell damage or, more rarely, meningeal hemorrhage, are not observed with either purified ET or LT and may reflect the action of additional virulence factors or the localized production of toxin at these sites during infection.

One of the most extensive and consistent necrotic lesions occurred in the cortex of the adrenal glands, characterized by hemorrhage and granulocytic infiltrates. Histopathological analyses of the adrenal medulla, however, did not reveal pathological lesions. The adrenal gland has several critical roles in maintaining body homeostasis. The glucocorticoids produced by the zona fasciculata have diverse functions including regulating glucose metabolism, cardiovascular function, inflammatory cytokine response, bone resorption/growth, and lymphocyte apoptosis.[39–42] Mineralcorticoids produced by the zona glomerulosa have a direct role in cardiac regulation as well as an indirect role through their critical function in maintaining osmotic homeostasis.[43] The adrenal medulla synthesizes catecholamines, which play an important role in the neuronal adrenergic response and have an effect on cardiac contractile rate and strength.[44] Determining which of these regulatory systems is perturbed, either by enhancement or loss of function, remains to be elucidated. Likewise, it will be important to determine whether the adrenal gland itself is a direct target of ET or whether ET acts further upstream in the hypothalamic-pituitary-adrenal axis.[44,45] Murine sex and strain differences in adrenal gland architecture and activity levels may potentially alter their response to ET.[46,47]

Lymphocytolysis was a consistent finding in all examined lymphoid tissue. Depletion of lymphocytes would impair the host's abilities to clear the bacterium and may represent a principal function for ET during the establishment of infection. Depletion of pluripotent stem cells from the bone marrow without necrotic debris and a corresponding neutrophilia and monocytosis in the blood suggests that cells were matured and mobilized into circulation. A stimulus for this event could be the large induction of G-CSF, a neutrophil progenitor cell maturation and activation factor, which may be due wholly or in part to a cAMP-responsive element found in the G-CSF promoter.[48] Recombinant G-CSF has been shown to induce neutrophilia in the blood of mice that likely originates from bone marrow or tissues.[49,50] Additionally, monocyte and neutrophil migration may be further acted on by the induction of the chemokines JE/MCP-1 and KC.[51] Consistent with tissue culture studies addressing ET-mediated cytokine response,[23,24] IL-6, but not TNF-α, was induced. At later time points IL-6, accompanied by an increase in JE/MCP-1 levels, is induced likely as a result of IL-1β release, a powerful inducer of these factors.[52]

Significant ET-mediated cardiac pathology was observed in these studies. Cardiovascular stress was reflected by the interstitial deposition of proteoglycans[53] as well as by thrombi formation within the ventricles and vessels. Cardiomyocyte degeneration was observed at later stages, occasionally encompassing broad areas of the heart. Telemetry measurements reveal bradycardia and hypotension after ET administration. Interestingly, a tachycardic response was absent in response to hypotension. Normally, profound hypotension is accompanied by compensatory tachycardia to maintain cardiac output, as was observed in anthrax patients.[2,3] The absence of this response combined with evidence of cardiac pathology suggests that ET may directly damage cardiomyocytes. As a result, ET-mediated lesions may prevent the tachycardic response that is expected from increases in cAMP, as is observed after stimulation of β-adrenergic receptors by administration of catecholamines or agonists such as isoproterenol.[54] More experimentation will be necessary to explain why ET does not induce a tachycardic response.

Few data are available as to the concentration of anthrax toxins in the blood of diseased animals. However, the similarity of pathological lesions displayed during inhalational anthrax disease in nonhuman primates and humans to many of those seen in our ET murine model demonstrates the usefulness of the reductionist approach taken here and in our previous studies[17] in distinguishing ET-mediated versus LT-mediated events. Because the bolus delivery of toxin serves to highlight potential targets of ET-mediated toxicity, it will be important in future studies to also explore continuous delivery models that may more closely mimic the natural course of disease.

The ET-mediated pathology we report here contrasts with that in a recent report in which BALB/c mice exposed to *B. anthracis* exhibited little pathology beyond pulmonary and splenic lesions and apparently did not present with pleural effusions or hemorrhage of the GI tract.[55] However, mice, unlike primates, are susceptible to *B. anthracis* strains that lack the toxin-encoding pX01 plasmid.[56] As a result, additional anthrax virulence factors such as capsule and hemolysins present in the murine spore model may cause death before toxin-mediated pathology develops.

These studies describe the widespread tissue destruction and murine mortality that results from exposure to ET. Whether the effects described here are principal targets of ET or secondary to perturbation of other systems remains to be elucidated. The acute damage done to bone, GI, lymphocytic, and cardiac systems suggests that ET

causes multiple organ failure in mice resulting in death. A greater understanding of ET-mediated toxicity will enable the development of therapies directed at disrupting this deadly component of anthrax toxin.

Acknowledgments

We thank Apolonio Concordia, Jorge Chavez, and Patricia Adzati for technical expertise and services in animal necropsies and sample processing; Dana Hsu for PA preparation; David Stephany for Luminex operation and data processing; Weisong He for construction and purification of the EF K346R mutant; and Dr. David Kleiner for critical review of the manuscript.

References

1. Turnbull PC: Introduction: anthrax history, disease and ecology. Curr Top Microbiol Immunol 2002, 271:1–19
2. Jernigan JA, Stephens DS, Ashford DA, Omenaca C, Topiel MS, Galbraith M, Tapper M, Fisk TL, Zaki S, Popovic T, Meyer RF, Quinn CP, Harper SA, Fridkin SK, Sejvar JJ, Shepard CW, McConnell M, Guarner J, Shieh WJ, Malecki JM, Gerberding JL, Hughes JM, Perkins BA: Bioterrorism-related inhalational anthrax: the first 10 cases reported in the United States. Emerg Infect Dis 2001, 7:933–944
3. Kuehnert MJ, Doyle TJ, Hill HA, Bridges CB, Jernigan JA, Dull PM, Reissman DB, Ashford DA, Jernigan DB: Clinical features that discriminate inhalational anthrax from other acute respiratory illnesses. Clin Infect Dis 2003, 36:328–336
4. Guarner J, Jernigan JA, Shieh WJ, Tatti K, Flannagan LM, Stephens DS, Popovic T, Ashford DA, Perkins BA, Zaki SR: Pathology and pathogenesis of bioterrorism-related inhalational anthrax. Am J Pathol 2003, 163:701–709
5. Barakat LA, Quentzel HL, Jernigan JA, Kirschke DL, Griffith K, Spear SM, Kelley K, Barden D, Mayo D, Stephens DS, Popovic T, Marston C, Zaki SR, Guarner J, Shieh WJ, Carver HW, Meyer RF, Swerdlow DL, Mast EE, Hadler JL: Fatal inhalational anthrax in a 94-year-old Connecticut woman. JAMA 2002, 287:863–868
6. Shafazand S, Doyle R, Ruoss S, Weinacker A, Raffin TA: Inhalational anthrax: epidemiology, diagnosis, and management. Chest 1999, 116:1369–1376
7. Leppla SH: Anthrax toxin. Bacterial Protein Toxins. Edited by Aktories K, Just I. Berlin, Springer, 2000, pp 445–472
8. Collier RJ, Young JAT: Anthrax toxin. Annu Rev Cell Dev Biol 2003, 19:45–70
9. Mourez M: Anthrax toxins. Rev Physiol Biochem Pharmacol 2004, 152:135–164
10. Duesbery NS, Webb CP, Leppla SH, Gordon VM, Klimpel KR, Copeland TD, Ahn NG, Oskarsson MK, Fukasawa K, Paull KD, Vande Woude GF: Proteolytic inactivation of MAP-kinase-kinase by anthrax lethal factor. Science 1998, 280:734–737
11. Vitale G, Bernardi L, Napolitani G, Mock M, Montecucco C: Susceptibility of mitogen-activated protein kinase kinase family members to proteolysis by anthrax lethal factor. Biochem J 2000, 352:739–745
12. Roberts JE, Watters JW, Ballard JD, Dietrich WF: Ltx1, a mouse locus that influences the susceptibility of macrophages to cytolysis caused by intoxication with Bacillus anthracis lethal factor, maps to chromosome 11. Mol Microbiol 1998, 29:581–591
13. Leppla SH: Anthrax toxin edema factor: a bacterial adenylate cyclase that increases cyclic AMP concentrations of eukaryotic cells. Proc Natl Acad Sci USA 1982, 79:3162–3166
14. Leppla SH: Bacillus anthracis calmodulin-dependent adenylate cyclase: chemical and enzymatic properties and interactions with eucaryotic cells. Advances in Cyclic Nucleotide and Protein Phosphorylation Research, vol 17. Edited by Greengard P. New York, Raven Press, 1984, pp 189–198
15. Drum CL, Yan SZ, Bard J, Shen YQ, Lu D, Soelaiman S, Grabarek Z, Bohm A, Tang WJ: Structural basis for the activation of anthrax adenylyl cyclase exotoxin by calmodulin. Nature 2002, 415:396–402
16. Tang WJ, Krupinski J, Gilman AG: Expression and characterization of calmodulin-activated (type I) adenylylcyclase. J Biol Chem 1991, 266:8595–8603
17. Moayeri M, Haines D, Young HA, Leppla SH: Bacillus anthracis lethal toxin induces TNF-α-independent hypoxia-mediated toxicity in mice. J Clin Invest 2003, 112:670–682
18. Ascenzi P, Visca P, Ippolito G, Spallarossa A, Bolognesi M, Montecucco C: Anthrax toxin: a tripartite lethal combination. FEBS Lett 2002, 531:384–388
19. Abramova FA, Grinberg LM, Yampolskaya OV, Walker DH: Pathology of inhalational anthrax in 42 cases from the Sverdlovsk outbreak of 1979. Proc Natl Acad Sci USA 1993, 90:2291–2294
20. Fritz DL, Jaax NK, Lawrence WB, Davis KJ, Pitt ML, Ezzell JW, Friedlander AM: Pathology of experimental inhalation anthrax in the rhesus monkey. Lab Invest 1995, 73:691–702
21. Vasconcelos D, Barnewall R, Babin M, Hunt R, Estep J, Nielsen C, Carnes R, Carney J: Pathology of inhalation anthrax in cynomolgus monkeys (Macaca fascicularis). Lab Invest 2003, 83:1201–1209
22. Grinberg LM, Abramova FA, Yampolskaya OV, Walker DH, Smith JH: Quantitative pathology of inhalational anthrax I: quantitative microscopic findings. Mod Pathol 2001, 14:482–495
23. Hoover DL, Friedlander AM, Rogers LC, Yoon IK, Warren RL, Cross AS: Anthrax edema toxin differentially regulates lipopolysaccharide-induced monocyte production of tumor necrosis factor alpha and interleukin-6 by increasing intracellular cyclic AMP. Infect Immun 1994, 62:4432–4439
24. Shen Y, Zhukovskaya NL, Zimmer MI, Soelaiman S, Bergson P, Wang CR, Gibbs CS, Tang WJ: Selective inhibition of anthrax edema factor by adefovir, a drug for chronic hepatitis B virus infection. Proc Natl Acad Sci USA 2004, 101:3242–3247
25. Pezard C, Berche P, Mock M: Contribution of individual toxin components to virulence of Bacillus anthracis. Infect Immun 1991, 59:3472–3477
26. Brossier F, Weber-Levy M, Mock M, Sirard JC: Role of toxin functional domains in anthrax pathogenesis. Infect Immun 2000, 68:1781–1786
27. Stanley JL, Smith H: Purification of factor I and recognition of a third factor of anthrax toxin. J Gen Microbiol 1961, 26:49–66
28. Yahr TL, Vallis AJ, Hancock MK, Barbieri JT, Frank DW: ExoY, an adenylate cyclase secreted by the Pseudomonas aeruginosa type III system. Proc Natl Acad Sci USA 1998, 95:13899–13904
29. Ladant D, Ullmann A: Bordetella pertussis adenylate cyclase: a toxin with multiple talents. Trends Microbiol 1999, 7:172–176
30. Soelaiman S, Wei BQ, Bergson P, Lee YS, Shen Y, Mrksich M, Shoichet BK, Tang WJ: Structure-based inhibitor discovery against adenylyl cyclase toxins from pathogenic bacteria that cause anthrax and whooping cough. J Biol Chem 2003, 278:25990–25997
31. Moayeri M, Martinez NW, Wiggins J, Young HA, Leppla SH: Mouse susceptibility to anthrax lethal toxin is influenced by genetic factors in addition to those controlling macrophage sensitivity. Infect Immun 2004, 72:4439–4447
32. Wood BJ, DeFranco B, Ripple M, Topiel M, Chiriboga C, Mani V, Barry K, Fowler D, Masur H, Borio L: Inhalational anthrax: radiologic and pathologic findings in two cases. AJR Am J Roentgenol 2003, 181:1071–1078
33. Varughese M, Chi A, Teixeira AV, Nicholls PJ, Keith JM, Leppla SH: Internalization of a Bacillus anthracis protective antigen-c-Myc fusion protein mediated by cell surface anti-c-Myc antibodies. Mol Med 1998, 4:87–95
34. Luna LG: Histopathologic Methods and Color Atlas of Special Stains and Tissue Artifacts. Gaithersburg, American Histolabs, Inc., 1992
35. Chutkow WA, Pu J, Wheeler MT, Wada T, Makielski JC, Burant CF, McNally EM: Episodic coronary artery vasospasm and hypertension develop in the absence of Sur2 K(ATP) channels. J Clin Invest 2002, 110:203–208
36. Hinrichs CR, Singer A, Maldjian P, Abu-Judeh H, Dadarwala A: Inferior vena cava thrombosis: a mechanism of posttraumatic adrenal hemorrhage. AJR Am J Roentgenol 2001, 177:357–358
37. Loeb WF, Quimby FW: The Clinical Chemistry of Laboratory Animals. Philadelphia, Taylor & Francis, 1999
38. Sack DA, Sack RB, Nair GB, Siddique AK: Cholera. Lancet 2004, 363:223–233

39. Andrews RC, Walker BR: Glucocorticoids and insulin resistance: old hormones, new targets. Clin Sci (Lond) 1999, 96:513–523
40. Whitworth JA, Mangos GJ, Kelly JJ: Cushing, cortisol, and cardiovascular disease. Hypertension 2000, 36:912–916
41. Webster JI, Tonelli L, Sternberg EM: Neuroendocrine regulation of immunity. Annu Rev Immunol 2002, 20:125–163
42. Cooper MS: Sensitivity of bone to glucocorticoids. Clin Sci (Lond) 2004, 107:111–123
43. Ngarmukos C, Grekin RJ: Nontraditional aspects of aldosterone physiology. Am J Physiol 2001, 281:E1122–E1127
44. Pepe S, van den Brink OW, Lakatta EG, Xiao RP: Cross-talk of opioid peptide receptor and beta-adrenergic receptor signalling in the heart. Cardiovasc Res 2004, 63:414–422
45. Rees DA, Scanlon MF, Ham J: Adenosine signalling pathways in the pituitary gland: one ligand, multiple receptors. J Endocrinol 2003, 177:357–364
46. Tanaka S, Matsuzawa A: Comparison of adrenocortical zonation in C57BL/6J and DDD mice. Exp Anim 1995, 44:285–291
47. Jones BC, Sarrieau A, Reed CL, Azar MR, Mormede P: Contribution of sex and genetics to neuroendocrine adaptation to stress in mice. Psychoneuroendocrinology 1998, 23:505–517
48. Hareng L, Meergans T, von Aulock S, Volk HD, Hartung T: Cyclic AMP increases endogenous granulocyte colony-stimulating factor formation in monocytes and THP-1 macrophages despite attenuated TNF-alpha formation. Eur J Immunol 2003, 33:2287–2296
49. Tamura M, Hattori K, Nomura H, Oheda M, Kubota N, Imazeki I, Ono M, Ueyama Y, Nagata S, Shirafuji N, Asano S: Induction of neutrophilic granulocytosis in mice by administration of purified human native granulocyte colony-stimulating factor (G-CSF). Biochem Biophys Res Commun 1987, 142:454–460
50. Basu S, Dunn A, Ward A: G-CSF: function and modes of action. Int J Mol Med 2002, 10:3–10
51. Gillitzer R, Goebeler M: Chemokines in cutaneous wound healing. J Leukoc Biol 2001, 69:513–521
52. Borish LC, Steinke JW: 2. Cytokines and chemokines. J Allergy Clin Immunol 2003, 111:S460–S475
53. Heeneman S, Cleutjens JP, Faber BC, Creemers EE, van Suylen RJ, Lutgens E, Cleutjens KB, Daemen MJ: The dynamic extracellular matrix: intervention strategies during heart failure and atherosclerosis. J Pathol 2003, 200:516–525
54. Taniguchi T, Fujiwara M, Ohsumi K: Possible involvement of cyclic adenosine 3′:5′-monophosphate in the genesis of catecholamine-induced tachycardia in isolated rabbit sinoatrial node. J Pharmacol Exp Ther 1977, 201:678–688
55. Lyons CR, Lovchik J, Hutt J, Lipscomb MF, Wang E, Heninger S, Berliba L, Garrison K: Murine model of pulmonary anthrax: kinetics of dissemination, histopathology, and mouse strain susceptibility. Infect Immun 2004, 72:4801–4809
56. Welkos SL: Plasmid-associated virulence factors of non-toxigenic (pX01-) Bacillus anthracis. Microb Pathog 1991, 10:183–198